

Color Restoration in Turbid Medium

Nimisha T M

IIT Madras

ee13d037@ee.iitm.ac.in

Karthik Seemakurthy

IIT Madras

ee13d037@ee.iitm.ac.in

A N Rajagopalan

IIT Madras

raju@ee.iitm.ac.in

Narayanaswamy

Vedachalam

National Institute of Ocean

Technology

veda@niot.res.in

Ramesh Raju

National Institute of Ocean

Technology

rramesh@niot.res.in

ABSTRACT

Light scattering and color distortions are two major issues with underwater imaging. Scattering occurs due to turbidity of the medium and color distortions are caused by differential attenuation of wavelengths as a function of depth. As a result, underwater images taken in a turbid medium have low contrast, color cast, and color loss. The main objective of this work is color restoration of underwater images i.e., produce its equivalent image as seen outside of the water surface. As a first step, we account for low contrast by employing dark channel prior based dehazing. These images are then color corrected by learning a mapping function between a pair of color chart images, one taken inside water and another taken outside. The mapping thus learned is with respect to a reference distance from the water surface. We also propose a color modulation scheme that is applied prior to color mapping to accommodate the same mapping function for different depths as well. Color restoration results are given on several images to validate the efficacy of the proposed methodology.

CCS Concepts

• Computing methodologies → Image processing;

Keywords

Color mapping, color modulation, white balancing, boosting, dehazing.

1. INTRODUCTION

Understanding and investigating underwater activities using images has been gaining popularity over the past few years. Classical image processing tools fail in underwater scenarios due to variations in optical properties of water. Water being dense, light gets attenuated and scatters more as compared to its transport in air. These effects are directly

responsible for image degradations in the form of blur, contrast loss, color cast and color loss.

Scattering is caused either due to suspended particles or due to turbidity in the medium. This induces color cast and haze to the captured images. Attenuation occurs due to absorption of light rays, as they travel through a medium. Different wavelengths of light get attenuated differently in water and hence the light reflected from the object inside water has different attenuation factors across the visible spectrum. Red undergoes severe attenuation followed by green, while blue is the least attenuated and penetrates the most. The net result is color loss. True color plays a very important role while analyzing specimens found in water. In this paper, we initially mitigate the effect of color cast and haze, and proceed to develop an approach for color correction which compensates for color loss in underwater images.

Several methods already exist for color correction of terrestrial images. These include intensity normalization [7], radiometric correction [17], white-balancing to a canonical illumination, and color correction [20]. A detailed survey on different color balancing techniques can be found in [10]. However, these methods fail to deliver good results on underwater images if employed as is. Methods have been developed in the literature that are specifically tailored to handle underwater degradations. In the literature, three types of approaches are prevalent for color correction of underwater images captured in turbid scenarios. These are enhancement based, dehazing based and sensor based.

Inspired by color and lightness constancy mechanisms of the human visual system, Chambah et al. [4] proposed an automatic color equalization approach to balance colors in underwater images. Luz et al. [21] proposed an MRF based approach where the color correction is considered as a task of assigning color to each node in the graph which best describes the surroundings. The parameters of MRF model are learnt from an image pair consisting of color corrected and color depleted patches. Bazeille et al. [2] use a series of image enhancement filters to improve edge visibility and contrast. Color restoration is done through linear translation of the histogram. Iqbal et al. [12] propose a two-stage approach consisting of histogram equalization of RGB channels followed by stretching of saturation and intensity channels of HSI to increase true color and to solve the lightness problem. Marine snow limits the performance of conventional color correction algorithms due to its shiny appearance. Boffety et al. [3] propose a modified histogram

ACM acknowledges that this contribution was authored or co-authored by an employee, contractor or affiliate of a national government. As such, the Government retains a nonexclusive, royalty-free right to publish or reproduce this article, or to allow others to do so, for Government purposes only.

ICVGIP '16 Guwahati, Assam India

© 2016 ACM. ISBN 978-1-4503-4753-2/16/12...\$15.00

DOI: <http://dx.doi.org/10.1145/3009977.3010028>

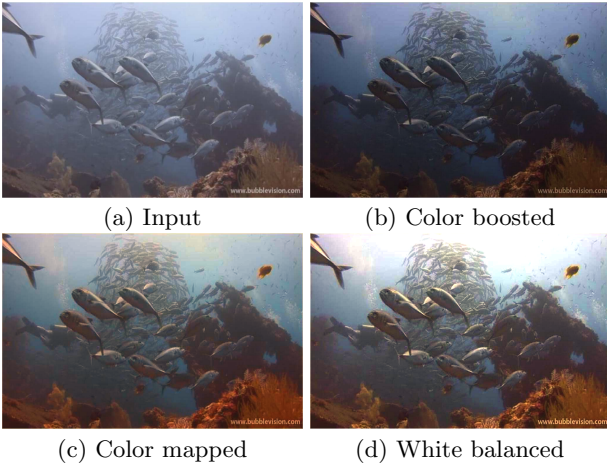


Figure 1: Proposed method: The input image (a) is first dehazed and then subjected to color modulation (b) and color mapping (c) followed by white balancing (d) to restore the lost colors.

stretching method which can restore the color of underwater images in the presence of snow.

Images captured in haze or fog experience severe contrast loss. Based on the nature of water and particulates in water, the light gets scattered and results in color cast. Hence, modeling of color cast can be done akin to atmospheric haze and the dark channel prior has been advocated for restoring the images. Among such dehazing based approach, Lu et al. [15] proposed a spectral-characteristic based color correction algorithm to recover the distorted color. Based on the fact that different wavelengths get attenuated differently inside water, Chiang et al. [5] proposed a wavelength compensation and dehazing technique to restore color as well as illumination. Fahimeh et al. [9] employs dictionary learning for underwater images. However, they use dictionary mainly for removing blurring artifacts and perform color cast removal using a modified version of the gray world algorithm. Li et al. [14] performs dehazing and red channel correction (using gray world assumption). While we also handle color cast, our main focus is color correction which involves taking into account depth-dependent wavelength attenuation.

Most of the ocean expeditions are performed by using remotely operated vehicles which are fitted with depth sensors [18] [19] [1]. True color correction can be done only if we know the absolute depth. Hence, approaches that employ depth sensors are more accurate than enhancement and dehazing based techniques. Kaeli et al. [13] propose a technique which compensates for the color by using the depth information from doppler velocity log as well as estimating attenuation coefficients of light in water. Vasilescu et al. [22] built a hardware which can compensate for color loss based on the measured distance.

In this paper, we propose a framework for restoration of colors in turbid underwater imagery. We propose a learning based technique in which we learn a mapping between a pair of images for a reference depth. The image pair consists of a color chart taken under the water surface and its corresponding pair taken outside water surface. Visibility loss due to turbidity is accounted for by dehazing using dark

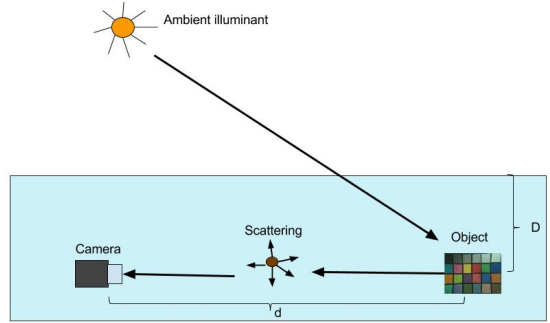


Figure 2: Underwater image formation.

channel prior. The dehazed image is further color corrected using the learned mapping. When there are depth changes from the reference, a color modulation technique is applied prior to color mapping to match the reference depth. In Fig. 1, the input image in (a) was captured at a depth different from the reference depth. Hence it is subjected to color modulation (b) prior to applying color correction (c) and white balancing (d). In the final result (Fig. 1(d)), the bluish tint is removed (when compared to the input) and colors properly restored.

Our main contributions are as follows

- We perform color correction of underwater images taken in turbid medium. Post correction, the recovered colors resemble their equivalent outside the water surface.
- We achieve the above by learning a color mapping between colors of a color chart taken inside and outside water. The mapping is learned for a reference depth.
- To accommodate different depths, we propose a color modulation scheme that is applied prior to color mapping.
- Our approach is the first of its kind to use color mapping for color correction in turbid water.

In Section 2, we describe underwater image formation. The proposed mapping based color correction scheme is discussed in Section 3. This is followed by quantitative and qualitative results in Section 4. We conclude with Section 5.

2. IMAGE FORMATION

In this section, we will briefly discuss the underwater image formation model used in this work. Fig 2 gives an illustration of the model. Throughout our discussions, we shall assume ambient light source alone. The effect of any external illuminant is not incorporated into the model. The image formation models in [8], [6] consider the effect of light scattering during the course of propagation from water surface to the object as well as from the object to the camera. A light beam with energy E_λ^A gets attenuated with respect to the distance D traveled from the water surface to the object surface. This attenuated ray is reflected from the object surface based on the surface reflectivity ρ of the object as $E_\lambda^A(x)N_{rer}(\lambda)^{D(x)}\rho_\lambda(x)$. This reflected light has to cover a distance of d to the camera during which it encounters attenuation again. The image will further get affected by water

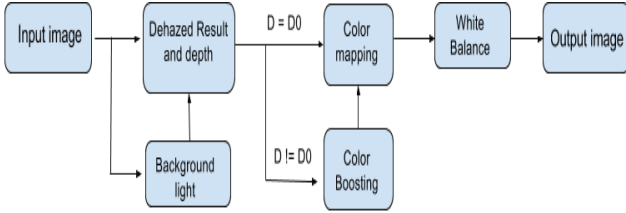


Figure 3: Flowchart of proposed method.

turbidity. The scattering of light increases with turbidity leading to haze in the captured images. Haze is a bottleneck as it reduces visibility and results in low contrast. The observed image I at a pixel location x is modeled as

$$I_\lambda(x) = (E_\lambda^A(x)N_{rer}(\lambda)^{D(x)}\rho_\lambda(x))N_{rer}(\lambda)^{d(x)} + (1 - N_{rer}(\lambda)^{d(x)})A_\lambda \quad (1)$$

where $\lambda \in \{R, G, B\}$, $N_{rer}(\lambda)$ is the attenuation factor (normalized energy ratio) encountered at different wavelengths and A_λ is the homogeneous background light. This can be equated to the hazy image formation model in [11] given by

$$I_\lambda(x) = J_\lambda(x)t_\lambda(x) + (1 - t_\lambda(x))A_\lambda \quad (2)$$

where $J_\lambda(x)$ is the scene radiance at point x and $t_\lambda(x)$ is the residual energy ratio of $J_\lambda(x)$ reaching the camera after reflecting from the point x . From Eq. (1) and (2) it can be noted that $t_\lambda(x)$ is a function of both wavelength and the object to camera distance $d(x)$ and it can be written in terms of the attenuation factor $N_{rer}(\lambda)$ as

$$\begin{aligned} t_\lambda(x) &= e^{-\beta_\lambda d(x)} \\ &= N_{rer}(\lambda)^{d(x)} \end{aligned} \quad (3)$$

where β_λ is the attenuation coefficient corresponding to each wavelength. Based on the water type, the normalized energy ratio $N_{rer}(\lambda)$ can be given as

$$\begin{aligned} N_{rer}(\lambda) &= 0.83 \sim 0.85 \quad if \quad \lambda \in R \\ &= 0.93 \sim 0.97 \quad if \quad \lambda \in G \\ &= 0.95 \sim 0.99 \quad if \quad \lambda \in B \end{aligned}$$

3. MAPPING FOR COLOR CORRECTION

We propose here a mapping based method for color restoration of underwater images. The learning is done only once for a pair of color charts corresponding to underwater image at reference depth D_0 . When the incoming image is from the same reference depth, it is first subjected to dehazing to remove the scattering effects. The dehazed image is then color corrected using color mapping. White balancing is performed on the color mapped image in order to remove any remaining color casts. If the input underwater image is from a different depth D ($\neq D_0$), it is color modulated to the reference depth D_0 prior to color mapping. A flowchart of the proposed method is shown in Fig. 3. The steps involved in the process are explained below in detail.

3.1 Dehazing and depth estimation

Classical approaches on depth estimation from an image pair work by utilizing cues such as parallax, blur etc. In hazy environments, haze is directly proportional to depth, and

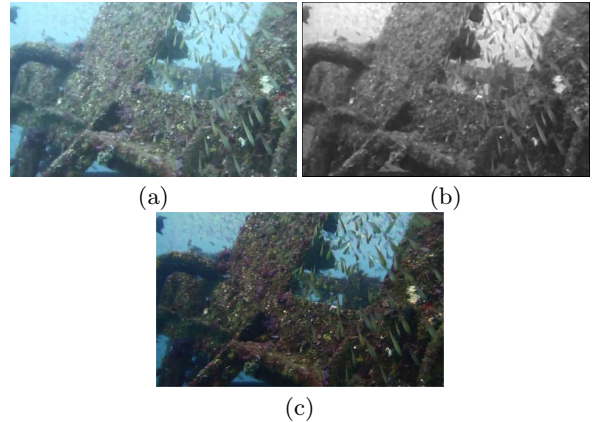


Figure 4: Result of dehazing: (a) Input image affected by haze and color distortions. (b) Estimated depth $d(x)$. (c) Result of dehazing.

hence can itself be used as a cue for depth. The dark channel prior (DCP) [11], can adequately quantify the concentration of haze in terrestrial images and has been used to infer scene depth in hazy environments. It is based on the central idea that in most non-sky patches, at least one color channel has very low intensity. The assumptions made in DCP are valid for underwater images as well i.e; at least one color channel has pixel intensity close to zero. DCP has been widely used in dehazing of underwater images too [6], [16].

The reflected light from a point x is given as

$$\begin{aligned} J_\lambda(x) &= E_\lambda^A(x)N_{rer}(\lambda)^{D(x)}\rho_\lambda(x) \\ &= \frac{I_\lambda(x) - (1 - N_{rer}(\lambda)^{d(x)})A_\lambda}{N_{rer}(\lambda)^{d(x)}} \end{aligned} \quad (4)$$

Now the dark channel for an underwater image can be defined as

$$J_{dark}(x) = \min_{\lambda} \min_{y \in \Omega(x)} J_\lambda(y) \quad (5)$$

where $\Omega(x)$ is a patch around the pixel x . As per dark channel prior, the assumption holds that at least one channel has intensity close to zero and that channel is the dark channel. Hence, $J_{dark}(x) \approx 0$. Taking the min operation in local patches on the observed image in Eq. (1) gives

$$\min_{y \in \Omega(x)} I_\lambda(y) = \min_{y \in \Omega(x)} J_\lambda(y)N_{rer}(\lambda)^{d(y)} + (1 - N_{rer}(\lambda)^{d(y)})A_\lambda \quad (6)$$

For a local patch around x , $N_{rer}(\lambda)^{d(y)}$ is a constant and is approximately equal to that at x . Taking one more min operation with respect to λ on both sides gives

$$\begin{aligned} \min_{\lambda} \min_{y \in \Omega(x)} I_\lambda(y) &= J_{dark}(x)N_{rer}(\lambda)^{d(x)} + \\ &\quad \min_{\lambda}(1 - N_{rer}(\lambda)^{d(x)})A_\lambda \end{aligned} \quad (7)$$

The first term in the RHS is approximately zero (due to DCP) and the above equation can be rearranged as

$$\min_{\lambda}(N_{rer}(\lambda)^{d(x)}) = 1 - \min_{\lambda} \left(\frac{\min_{y \in \Omega(x)} I_\lambda(y)}{A_\lambda} \right) \quad (8)$$

The homogeneous background light refers to the brightest pixel intensity in the image. But this might go wrong in the

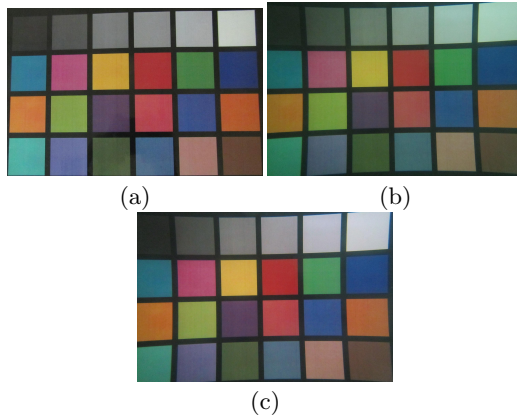


Figure 5: Color mapping. (a) Reference image taken outside the water surface. (b) Input image taken underwater. (c) Result of color mapping applied to (b).

presence of shining surface in the observed image. Hence, the input hazy image is first subjected to local minima operation in local patches and the background light is defined as the maximum intensity among all the local minima.

$$A_\lambda = \max_{x \in I} \min_{y \in \Omega(x)} I_\lambda(y) \quad (9)$$

Given the background light and $N_{rer}(R)$, the object to camera distance $d(x)$ can be calculated using Eq. (8). The dehazed image $J_\lambda(x)$ can then be estimated using Eq. (4). Fig. 4 shows an example of dehazing. The recovered depthmap and the haze removed image are shown respectively in Figs. 4(b) and (c).

3.2 Color mapping

The goal of color mapping is to map colors from a source to a target image. A scene imaged under different situations will show color variations depending upon the surrounding illumination as well as the characteristics of the imaging device used. A mapping function f can be found in such situations that maps the colors from a standard color chart (taken with a camera under some illuminant) to the required reference colors (as seen from a particular camera under some particular illuminant). But these functions are specific to the illuminants and cameras. It has to be relearned whenever the camera or illuminant changes.

Here we employ color mapping to map from a dehazed image in underwater to that of its equivalent taken outside the water surface. This mapping is specific for an object to water surface distance D . We learn this mapping for a color chart pair taken inside and outside the water surface.

The mapping can be written as a transform T which when applied on the RGB value from input will give the corresponding RGB value of the reference image. For a linear mapping, the dimension of T turns out to be 3×3 . Instead, we consider a polynomial model of degree n where $n \leq 10$. Hence, our transform matrix is a $3 \times n$ matrix. This transform is learned using M corresponding pixels from the color charts taken under the two conditions described earlier. The higher order terms considered are $[r, g, b, rg, rb, gb, r^2, g^2, b^2, rgb]^T$. Let the reference image's pixel intensity be col-



Figure 6: Change in observed colors with distance from water surface.

lected in a matrix $R_{3 \times M}$ and its corresponding intensity with its higher orders from the source image be collected in matrix $S_{n \times M}$. The mapping can then be written as

$$R_{3 \times M} = T_{3 \times n} S_{n \times M} \quad (10)$$

There are $3n$ unknowns to be solved. Hence, we need at least $M = 3n$ unique correspondences. Since we have color charts imaged under both conditions, we pick $M >> 3n$ correspondences and solve an over determined system of equations. Eq. (10) can be rewritten in the form of $y = Ax$ as shown in Eq. (11) and solved using least squares method as $x = (A^T A)^{-1} A^T y$.

$$\begin{pmatrix} r_1 & g_1 & .. & b_1^2 & r_1 g_1 b_1 & 0_{1 \times n} & 0_{1 \times n} \\ 0_{1 \times n} & r_1 & g_1 & .. & b_1^2 & r_1 g_1 b_1 & 0_{1 \times n} \\ 0_{1 \times n} & 0_{1 \times n} & r_1 & g_1 & .. & b_1^2 & r_1 g_1 b_1 \\ .. & .. & .. & .. & .. & .. & .. \end{pmatrix}_{3M \times 3n} * \\ \begin{pmatrix} T_{11} \\ T_{12} \\ .. \\ T_{1n} \\ .. \\ T_{31} \\ .. \\ T_{3n} \end{pmatrix}_{3n \times 1} = \begin{pmatrix} R_1 \\ G_1 \\ B_1 \\ .. \\ R_M \\ G_M \\ B_M \end{pmatrix}_{3M \times 1} \quad (11)$$

Fig. 5 our result for color mapping. Figs. 5(a) and (b) are the two corresponding images taken outside and inside water surface, respectively. The mapping is learned between these two images and is used to map the colors from an underwater image to that of the reference image outside water. The obtained result after color mapping is shown in Fig. 5(c). The mapped colors closely resemble their equivalent taken outside the water surface (Fig. 5(a)).

3.2.1 White Balancing

White balancing is used to remove unrealistic color casts from the captured images. It works with the assumption that there is at least one white point in the captured image. There are different methods of white balancing such as gray world, shades of gray, white patch algorithm etc. We used the gray world algorithm which assumes that average reflectance of a scene is gray. It works by equalizing the means of all the color channels. It keeps the green channel as reference and multiplies the means of other channels with a gain factor such that all the means become equal. Let R_m, G_m and B_m be the means of the three color channels.

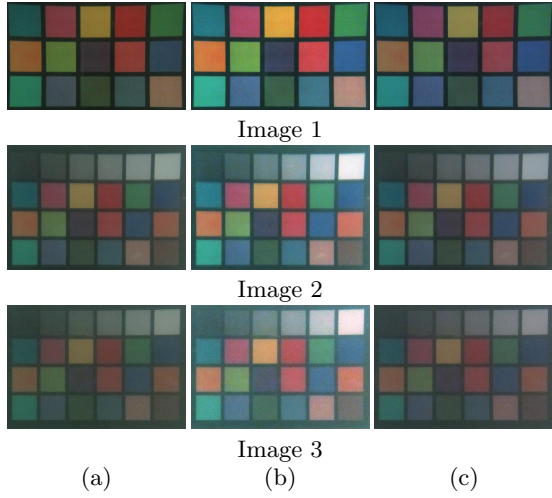


Figure 7: Quantitative results for color charts at same reference depth but different object to camera distances. All of these images are captured in clear water without turbidity. The reference image taken outside water is given in Fig 5(a). (a) Input image. (b) Our result. (c) Result obtained by directly white balancing (DWB) the input.

Then the white balanced image is given by

$$\begin{aligned} R_w(x, y) &= \frac{G_m}{R_m} R(x, y) \\ G_w(x, y) &= G(x, y) \\ B_w(x, y) &= \frac{G_m}{B_m} B(x, y) \end{aligned} \quad (12)$$

We apply white balancing post color mapping to remove any unwanted color casts that can result due to mapping errors.

Table 1: Quantitative analysis (PSNR in dB).

Image	Input	Our result	DWB
1	16.03	23.68	18.9
2	16.1	20.01	17.8
3	15.47	19.1	16.4

3.3 Color Modulation

The discussions till now tacitly assumed the distance from water surface to the object to be constant. Let this distance be the reference depth D_0 . This is the depth for which the color mapping was learned between the color charts. (This mapping is fixed and is used on all the examples in the paper.) When the water column depth changes, this mapping no longer holds. With increase or decrease in the depth, the attenuation encountered by the light beam changes and the observed colors will change. The effect of change in D on the observed colors can be seen from Fig. 6. As depth increases, the light rays get attenuated and only the wavelength corresponding to blue dominates.

Since the learning was done for reference depth D_0 , an image obtained at any other depth level (say D_1) is first dehazed to obtain the scene radiance J . The scene radiance is dependent on the scene depth as can be seen from Eq.

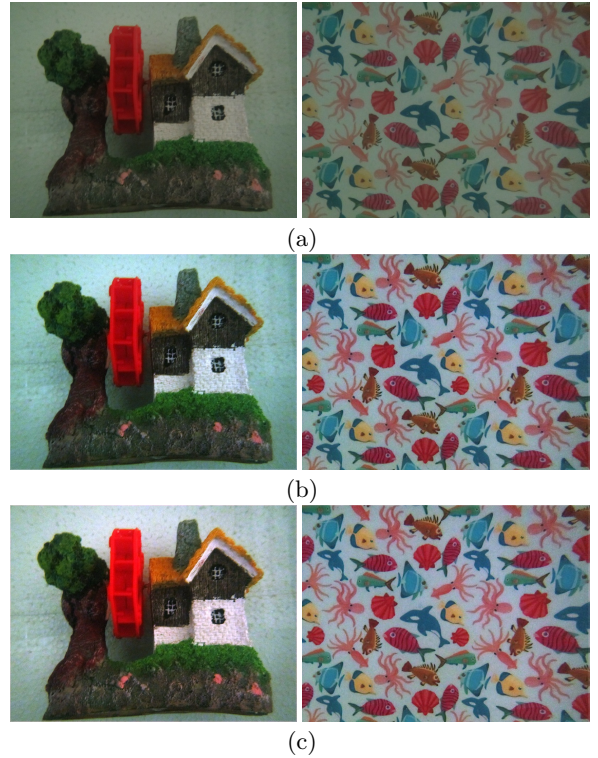


Figure 8: Experiments on images taken at same reference depth and with little turbidity. (a) Input images. (b) Color corrected result. (c) Final result after white balancing (b).

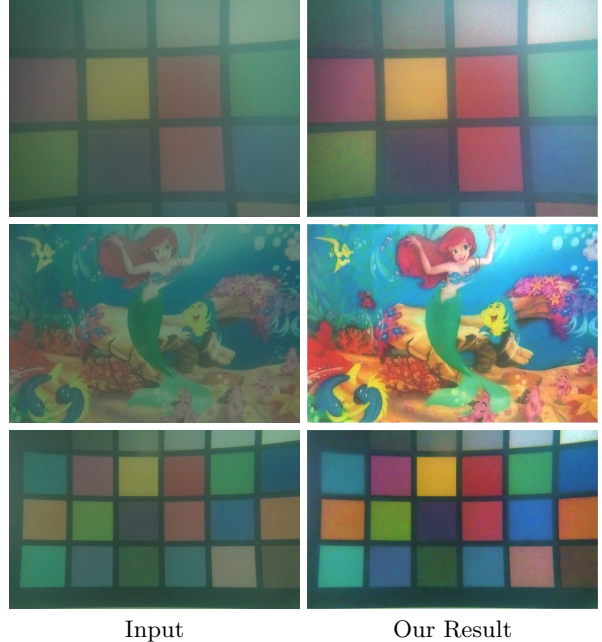


Figure 9: Experiments on images taken at same reference depth but with higher turbidity.

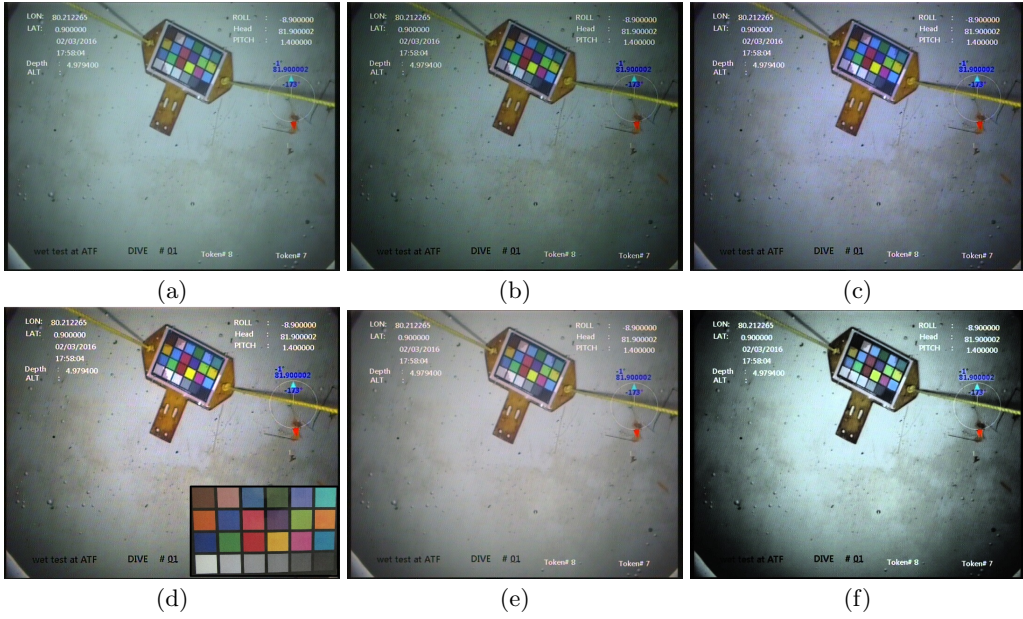


Figure 10: Input from different depth D . (a) Input. (b) Color modulated image. (c) Output of color mapping. (d) The bluish tint in (c) is removed by white balancing. (e) Result obtained by directly white balancing the input in (a). (f) Result obtained by histogram equalization of the input in (a).

(4). Hence the radiance image is first color-modulated to the reference depth prior to applying the color mapping. Let the observed scene radiance at D_0 be J_0 and at depth D_1 be J_1 . Suppose $D_1 > D_0$. Then the modulation is done as follows

$$\begin{aligned} J_{0\lambda} &= E_\lambda^A N_{rer}(\lambda)^{D_0} \rho_x \\ J_{1\lambda} &= E_\lambda^A N_{rer}(\lambda)^{D_1} \rho_x \end{aligned} \quad (13)$$

We need to boost J_1 to J_0 and it is given as

$$J_{0\lambda} = J_{1\lambda} N_{rer}(\lambda)^{D_0 - D_1} \quad (14)$$

Since the decay coefficients are < 1 and the power term is negative, this boosts up each channel strength towards the reference frame.

4. EXPERIMENTAL RESULTS

The performance of our learning based color correction scheme is evaluated both quantitatively and qualitatively using images captured under different depths and object to camera distances. The experiments are mainly performed in an aquarium and in an indoor tank. Some results are also shown on images taken from [6]. The aquarium is of size $120 \text{ cm} \times 60 \text{ cm} \times 50 \text{ cm}$ so we could get a maximum reference depth D_0 of 50 cm. The indoor tank has a depth of 7 meters.

4.1 Quantitative Analysis

A quantitative analysis of the proposed algorithm is made by color correcting the captured images of color charts at different object to camera distances. The input images of Fig. 7 are taken at an object to camera distance of 35, 55 and 81 cm, respectively. These inputs are subjected to dehazing, color mapping and white balancing to obtain the color corrected results in Fig. 7(b). The result of directly white

balancing (DWB) the input is also shown for each of these inputs in Fig. 7(c). The results obtained are then compared with the reference color chart taken outside the water surface (Fig. 5(a)). Quantitative measure based on PSNR is provided in Table 1. It is quite evident from Fig. 7 and the quantitative evaluation in Table 1 that the color restoration efficiency of our method is far better as compared to just white balancing. As the object to camera distance is increased, light rays reflecting from the object undergo more attenuation. The colors with red tint get attenuated more and some of the colors having red in them are indistinguishable as can be seen from the input in the bottom row of Fig. 7. But these colors are correctly recovered and are distinguishable in our results (Fig. 7(b)).

4.2 Real Experiments

We begin with experiments on images captured in mild turbidity. These images were captured at the same reference depth for which the mapping was learned for. Even though the effect of haze due to turbidity is less for these images, the effect of scattering cannot be neglected in underwater imaging. Hence, we dehaze these inputs as well. Fig. 8 shows the result obtained by our method on two sets of images taken under the same acquisition conditions. The color cast in the input is due to light attenuation. The color corrected final result after white balancing the color mapped images are shown in the last row. The final result (Fig. 8(c)) is well-enhanced in colors and the color cast is almost completely removed by our method.

We also verified the performance of our scheme in a more turbid scenario. It is common to emulate turbidity by adding a suitable quantity of milk. Fig. 9 shows the results of our method for such a scenario. The acquired images had color distortions as well as hazy appearance. Since the images captured were from the same reference depth, no color mod-

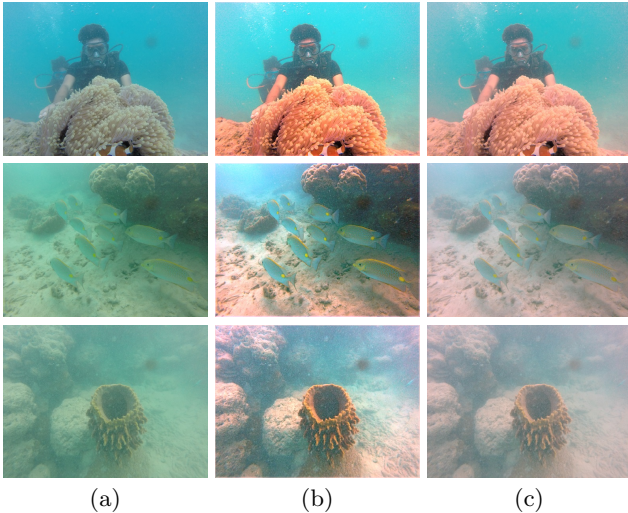


Figure 11: Additional results: (a) Input underwater images. (b) Result obtained by our method. (c) Result obtained by DWB.

ulation was done. The input was dehazed followed by color mapping and white balancing. The final result is provided in Fig. 9 along with the hazy input. The output has its colors and contrast recovered properly. The light red, pink and orange colors in the inputs were more or less similar in appearance but these are restored correctly by our method.

To show the efficacy of color modulation, we conducted our next experiment on images taken at a different depth from the reference. The input image in Fig. 10 is captured in a large water tank. Hence, the depth of these scenes is greater than the reference depth ($D > D_0$). The depth of the object from the water surface is 7 meter while the reference depth is only around 50 cm. Hence, prior to color mapping, color modulation is performed to boost the channel strength to that of the reference. The result of each step for the complete pipeline is shown in Fig. 10. The input is first dehazed and color boosted, and the result is shown in Fig. 10(b). This image is then subjected to color mapping. The color mapped image (Fig. 10(c)) had a color cast which is corrected by the white balancing step. The final result of our method is provided in Fig. 10(d). For purpose of comparison, the result of directly white balancing the input image is shown in Fig. 10(e). This result is not satisfactory as the colors are not properly mapped and have low contrast. The histogram equalized result is provided in Fig. 10(f) which is also not acceptable. It can be observed here that the contrast has increased significantly but the restored image has unnatural colors. Compared to these two methods, the colors are significantly better restored in our result. Please refer to the inset image shown in Fig. 10(d) which is captured outside the water surface to visually verify the restored colors.

Three more sets of additional results are provided in Fig. 11 to show the importance of our color modulation scheme. These are scuba diving images. The input images are first dehazed and then color modulated using the prior information that these were captured at a depth of about 8 meters from the water surface. The final results obtained for these input images are shown in Fig. 11(b). For comparison,

we also provide the result of DWB in Fig. 11(c). White balancing the input as such removes the color cast but the recovered images have less contrast and the colors are not restored properly; whereas our method removes the color cast and restores the colors as well.

Comparisons with other correcting methods are shown in Fig. 12. The comparison results shown in Figs. 12 (b),(c) and (e) are based on chromatic dehazing, histogram equalization and wavelength compensation (WCID) methods, respectively, and are taken from [6]. The result of directly white balancing the input and the result of our mapping based color restoration method are shown in Figs. 12(d) and (f). It can be noticed here that our method performs on par with the state-of-art method in [6] (Fig. 12(e)), while computationally being more efficient. The method in [6] is basically a step-by-step inversion of the image formation model to retrieve the radiance, whereas our aim is to produce an equivalent of the underwater image as seen from outside the water surface which we achieve through dehazing, color modulation and color mapping. Additional results and comparisons are provided in supplementary material.

5. CONCLUSIONS

We proposed here a scheme for color restoration of underwater images taken in turbid medium. Turbidity leads to haziness in the captured images along with color loss. We employed the idea of color mapping and mapped the colors of an underwater image to its equivalent as seen from outside the water surface. The mapping is learned only once for a particular reference depth. We also proposed a color modulation module to enable the same mapping to be applicable at different depths. We also accounted for haze by using the dark channel prior. Both quantitative as well as qualitative results were provided on many examples.

6. ACKNOWLEDGMENT

Support provided by National Institute of Ocean Technology, Chennai, India through project sanction No. RB1516ELE011NIOTANRA is gratefully acknowledged.

7. REFERENCES

- [1] D. Alley, B. Cochenour, and L. Mullen. Remotely operated compact underwater temporally encoded imager: Cutei. In *SPIE Defense + Security*, pages 982708–982708. International Society for Optics and Photonics, 2016.
- [2] S. Bazeille, I. Quidu, L. Jaulin, and J.-P. Malkasse. Automatic underwater image pre-processing. In *CMM’06*, 2006.
- [3] M. Boffety and F. Galland. Phenomenological marine snow model for optical underwater image simulation: Applications to color restoration. In *2012 Oceans-Yeosu*, pages 1–6. IEEE, 2012.
- [4] M. Chambah, D. Semani, A. Renouf, P. Courtellemont, and A. Rizzi. Underwater color constancy: enhancement of automatic live fish recognition. In *Electronic Imaging 2004*, pages 157–168. International Society for Optics and Photonics.
- [5] J. Y. Chiang and Y.-C. Chen. Underwater image enhancement by wavelength compensation and

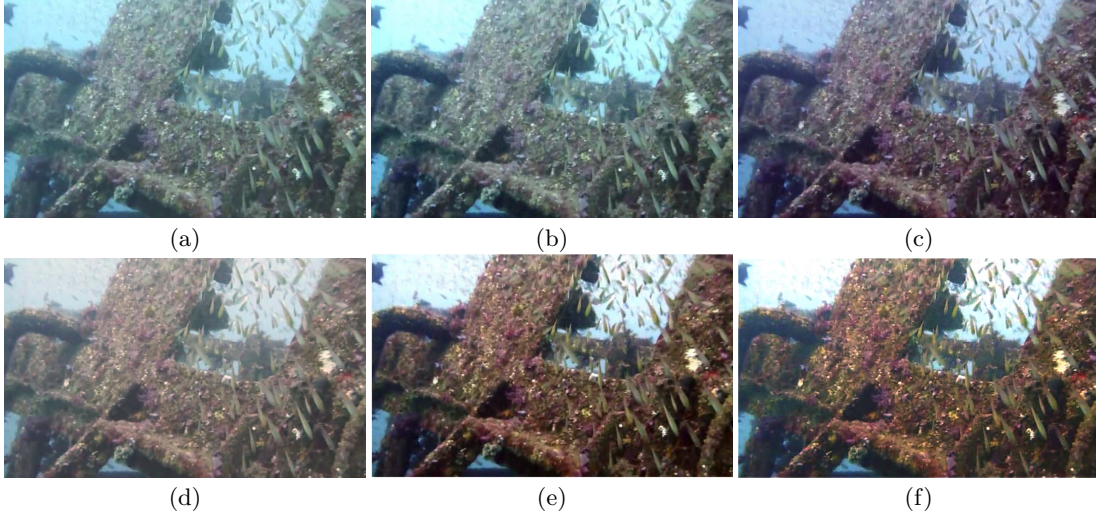


Figure 12: Comparisons (a) Input. (b) Image obtained after chromatism based dehazing. (c) Image obtained after histogram equalization. (d) Image obtained by direct white balancing of the input. (e) Result of WCID. (f) Our result.

- dehazing. *IEEE Transactions on Image Processing*, 21(4):1756–1769, 2012.
- [6] J. Y. Chiang, Y.-C. Chen, and Y.-F. Chen. Underwater image enhancement: using wavelength compensation and image dehazing (wcid). In *International Conference on Advanced Concepts for Intelligent Vision Systems*, pages 372–383. Springer, 2011.
- [7] X. Dai and S. Khorram. The effects of image misregistration on the accuracy of remotely sensed change detection. *IEEE Transactions on Geoscience and Remote sensing*, 36(5):1566–1577, 1998.
- [8] P. Drews, E. Nascimento, F. Moraes, S. Botelho, and M. Campos. Transmission estimation in underwater single images. In *Proceedings of the IEEE International Conference on Computer Vision Workshops*, pages 825–830, 2013.
- [9] F. Farhadifard, Z. Zhou, and U. F. von Lukas. Learning-based underwater image enhancement with adaptive color mapping. In *2015 9th International Symposium on Image and Signal Processing and Analysis (ISPA)*, pages 48–53. IEEE, 2015.
- [10] A. Gijsenij, T. Gevers, and J. Van De Weijer. Computational color constancy: Survey and experiments. *IEEE Transactions on Image Processing*, 20(9):2475–2489, 2011.
- [11] K. He, J. Sun, and X. Tang. Single image haze removal using dark channel prior. *IEEE transactions on pattern analysis and machine intelligence*, 33(12):2341–2353, 2011.
- [12] K. Iqbal, R. Abdul Salam, M. Osman, A. Z. Talib, et al. Underwater image enhancement using an integrated colour model. *IAENG International Journal of Computer Science*, 32(2):239–244, 2007.
- [13] J. W. Kaeli, H. Singh, C. Murphy, and C. Kunz. Improving color correction for underwater image surveys. In *OCEANS’11 MTS/IEEE KONA*.
- [14] C. Li, J. Quo, Y. Pang, S. Chen, and J. Wang. Single underwater image restoration by blue-green channels dehazing and red channel correction. In *2016 IEEE International Conference on Acoustics, Speech and Signal Processing (ICASSP)*, pages 1731–1735. IEEE, 2016.
- [15] H. Lu, Y. Li, L. Zhang, and S. Serikawa. Contrast enhancement for images in turbid water. *JOSA A*, 32(5):886–893, 2015.
- [16] S. Mallik, S. S. Khan, and U. C. Pati. Underwater image enhancement based on dark channel prior and histogram equalization. 2016.
- [17] S. Negahdaripour. Revised definition of optical flow: Integration of radiometric and geometric cues for dynamic scene analysis. *IEEE Transactions on Pattern Analysis and Machine Intelligence*, 20(9):961–979, 1998.
- [18] D. Sathianarayanan, R. Ramesh, A. N. Subramanian, G. Harikrishnan, D. Muthukumaran, M. Murugesan, E. Chandrasekaran, S. Elangovan, V. D. Prakash, A. Vadivelan, et al. Deep sea qualification of remotely operable vehicle (rosub 6000). In *Underwater Technology Symposium (UT)*, pages 1–7. IEEE, 2013.
- [19] A. Sundaresan. *Docking of underwater vehicle: Model, Autopilot design, and Guidance*. PhD thesis, TU Delft, Delft University of Technology, 2016.
- [20] J. Thomas, K. W. Bowyer, and A. Kareem. Color balancing for change detection in multitemporal images. In *Applications of Computer Vision (WACV), 2012 IEEE Workshop on*, pages 385–390. IEEE, 2012.
- [21] L. A. Torres-Méndez and G. Dudek. Color correction of underwater images for aquatic robot inspection. In *International Workshop on Energy Minimization Methods in Computer Vision and Pattern Recognition*, pages 60–73. Springer, 2005.
- [22] I. Vasilescu, C. Detweiler, and D. Rus. Color-accurate underwater imaging using perceptual adaptive illumination. *Autonomous Robots*, 31(2-3):285–296, 2011.